An analytical study of thermocapillary flow and surface deformations in floating zone

G. Chen, Bernard Roux

An analytical study of thermocapillary flow and surface deformations in floating zone

G. CHEN and B. ROUX

Institut de Mécanique des Fluides, UMR CNRS 34
1, rue Honnorat 13003 Marseille, France

Abstract—Small amplitude thermocapillary-driven convection and deformable free surface in a floating zone configuration with radiation and in the absence of gravity is considered. An analytical solution is constructed in the limit of small capillary number by expanding all fields in a power series in terms of capillary number. The first order approximation, a Stokes-type problem, is solved in terms of Papkovich–Fadle functions. The effect of Biot number and aspect ratio is examined. This analytical solution is compared with recent non-linear numerical calculations. The numerical solutions tend to the analytical ones, asymptotically as $Ma \to 0$. The comparison for increasing Ma, allowed us to precise the domain of validity of the analytical solution, for the surface temperature and the surface velocity.

INTRODUCTION

The floating zone method is widely used as a crystal growth process for high-purity semiconductor materials, such as silicon and germanium. The advantage of this technique is that container contamination can be eliminated, so the growing crystal is free to expand and is less likely to generate large thermoelastic stresses that lead to the generation of defects and dislocations. However, its application is limited on earth to the growth of crystals with diameters less than approximately 1 cm because deformation of the meniscus by gravity causes detachment of the melt from the crystal [1]. Since a microgravity environment provides the more stable hydrodynamic situation of reduced hydrostatic pressure and buoyancy convection, there appears the possibility of growing larger-diameter single crystals in a space laboratory. Such experiments have been planned at the beginning of the seventies. However, even in the absence of gravity the presence of a free melt–gas interface can lead to another type of convection, i.e. thermocapillary convections, which can have a decisive effect on the quality of the crystal. In particular, hydrodynamic instabilities associated with time-dependent (oscillatory) convection can promote undesirable dopant inhomogeneities in the growing crystals [2]. In the last 20 years, a great deal of research effort, including experimental, theoretical and numerical approaches, has been performed to understand this type of convection which is driven by surface tension gradients along the free interface. (Reviews of previous work are given in [3–5].) Although experimental and numerical progress has been made in determining the structure and stability range of the basic, steady, axisymmetric flow, only a few analytical results are available for floating zones. They are mainly for very simple geometrical configurations and boundary conditions. To our knowledge, Da-Riva and Pereira [6] were one of the first to present an analytical solution for the thermocapillary flows, but they only considered the case of half floating-zone in which the upper circular rod is maintained at higher temperature than the lower rod. They used a regular perturbation approach based on a small parameter, ϵ, which measures the deviation of the imposed temperature field from its mean value. They then obtained a reduced system (Stokes flow) that is solved in terms of a Papkovich–Fadle functions. This technique was first suggested in the work of Smith [7] and has been studied by Joseph *et al.* [8, 9], Napolitano and Golia [10], Napolitano *et al.* [11] and Davis [12]. Note that Kuhlmann [13] used the same idea to study small amplitude thermocapillary flow in a half floating-zone configuration. A comparison with nonlinear numerical calculations has been made. It has been shown that the analytical solutions are nearly identical to the numerical solutions for Reynolds number up to 100 for $Pr = 0.1$. In this paper an analytical solution for the flow field and surface deformation in a full floating-zone is also presented. The technique employed is the same method as [6, 13], but we consider more realistic thermal boundary conditions accounting for radiative heat transfer.

PROBLEM FORMULATION

Consider a floating zone confined between two coaxial cylindrical rods of radius R placed $2L$ apart, which is heated at the mid-height by an external ring heater with a specified ambient temperature distribution $T_a(z) = T_m + \Delta T \exp(-z^2/d^2)$ along the free surface, as shown in Fig. 1. The upper and lower solid–melt interfaces are assumed to be flat and they are kept at the melting point temperature T_m. The liquid volume is assumed to be $V = 2\pi R^2 L$ and the liquid–gas interface is described by a function $h(z)$, with $h(\pm 1) = R$ assuming fixed contact lines. The melt is bounded by a passive gas of negligible density

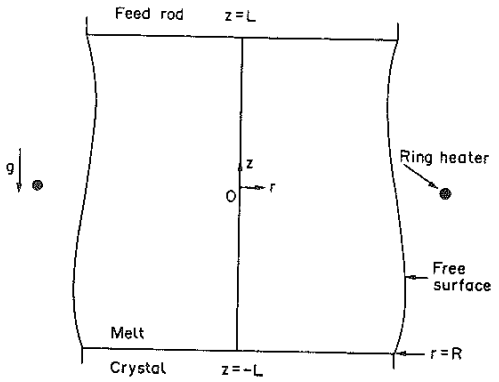

Fig. 1. Schematic representation of floating zone and associated coordinate system.

and viscosity. It is assumed, without loss of generality, that the pressure of the surrounding gas is constant. Even in absence of gravity, a flow is driven by thermocapillary force since the surface tension, σ, is assumed to linearly depend on the temperature

$$\sigma(T) = \sigma_0 - \gamma(T - T_m) \tag{1}$$

where σ_0 is the surface tension of the liquid at the melting temperature T_m and $\gamma = -\partial\sigma/\partial T$. Equation (1) is a good approximation for melt silicon [14]. If the temperature difference, $\Delta T = T_{heater} - T_m$, is small, the flow and surface deformation are steady and axisymmetric. Let us introduce a set of scales, respectively for length (r, z), velocity (u, w), pressure p, and temperature $(T - T_m)$,

$$L_{ref} = L,\ U_{ref} = \gamma\Delta T/\mu,\ p_{ref} = \gamma\Delta T/L,\ T_{ref} = \Delta T. \tag{2}$$

Then, the dimensionless equations for the radial velocity $u(r, z)$, axial velocity $w(r, z)$, pressure $p(r, z)$, temperature $T(r, z)$ and free surface $h(z)$ can be written in the form

$$u_r + r^{-1}u + w_z = 0, \tag{3a}$$

$$\mathrm{Re}(uu_r + wu_z) = -p_r + \nabla^2 u - r^{-2}u, \tag{3b}$$

$$\mathrm{Re}(uw_r + ww_z) = -p_z + \nabla^2 w, \tag{3c}$$

$$\mathrm{RePr}(uT_r + wT_z) = \nabla^2 T, \tag{3d}$$

where $\nabla^2 = \partial_r^2 + r^{-1}\partial_r + \partial_z^2$ and subscripts r and z denote partial derivatives ∂_r and ∂_z, respectively. The Reynolds and Prandtl numbers are defined by $\mathrm{Re} = \gamma\Delta T/\mu\nu$ and $\mathrm{Pr} = \nu/\alpha$, respectively. Marangoni number is denoted by $\mathrm{Ma} = \mathrm{RePr}$.

These equations are subjected to the following boundary conditions:

at the solid–melt interfaces $(z = -1,\ 1)$

$$u = w = T = 0 \tag{4a}$$

at the symmetric axis $(r = 0)$

$$u = w_r = T_r = 0. \tag{4b}$$

The only tangential force on the free surface is the thermocapillary one. A force balance at free surface, $r = h(z)$, leads to:

$$-p + 2N^{-2}[u_r - h_z w_r + h_z(-u_z + h_z w_z)] = Ca^{-1}(1 - CaT)[h_{zz}N^{-3} - h^{-1}N^{-1}] \tag{4c}$$

—tangential component:

$$(1 - h_z^2)(u_z + w_r) + 2h_z(u_r - w_z) = -N^{-1}(T_z + h_z T_r) \tag{4d}$$

where $N = (1 + h_z^2)^{1/2}$. Ca is the Capillary number, given by $\mathrm{Ca} = \gamma\Delta T/\sigma_0$, which measures the degree of deformation of the free surface; when $\mathrm{Ca} \to 0$ the deformation becomes asymptotically small.

The kinematic condition, i.e. the free boundary is a streamline, leads to

$$u = h_z w. \tag{4e}$$

The thermal boundary condition obtained from the energy balance at the free surface is

$$N^{-1}(T_r - h_z T_z) = -4\,\mathrm{Bi}(T - T_a),$$

with

$$T_a = \exp(-z^2/d^2), \tag{4f}$$

where Biot like number $\mathrm{Bi} = \epsilon\sigma^*(T_m)^3 L/\kappa$ measures the heat transfer between the melt and the heater [1].

Apart from the boundary conditions (4a)–(4f), the liquid must also satisfy the mass conservation constraint. Since the liquid is assumed to be incompressible, its total volume must remain constant, therefore the relation

$$\int_{-1}^{1} h^2(z)\,dz = 2/A \tag{4g}$$

must hold, where A is the aspect ratio, defined by $A = L/R$.

Finally, the fixed contact condition for the free boundary $h(z)$ at the melt–solid interfaces leads to

$$h(-1) = h(1) = 1/A. \tag{4h}$$

Equations (3) with boundary conditions (4) form the so-called free-boundary problem in which the location of the free surface $h(z)$ has to be determined as a part of the solution. Numerical simulations of this model problem have been conducted recently using a finite-difference method [15]. Here we are interested in generating mathematical expressions to describe the velocity and temperature fields and (small) surface deformation in the limit of small capillary number in an attempt to: (i) reveal the essential dynamics of the linear flow taking place in floating zones; (ii) use this analytical solution as the basic steady flow for a bifurcation analysis in view of determining the onset of time dependent thermocapillary convection. This last point is very important from point of view of crystal growth process. The analysis is generated by constructing a solution in the limit of vanishing capillary number $(\mathrm{Ca} \to 0)$ [16, 17].

ASYMPTOTIC SOLUTION

All fields are expressed in a power series in terms of capillary number

$$u(r, z) = \sum_{m=0}^{\infty} \mathrm{Ca}^m u_m(r, z) \tag{5a}$$

$$w(r, z) = \sum_{m=0}^{\infty} \mathrm{Ca}^m w_m(r, z), \tag{5b}$$

$$p(r,z) = \mathrm{Ca}^{-1} p_s + \sum_{m=0}^{\infty} \mathrm{Ca}^m p_m(r,z), \quad (5c)$$

$$T(r,z) = \sum_{m=0}^{\infty} \mathrm{Ca}^m T_m(r,z), \quad (5d)$$

$$h(z) = h_s + \sum_{m=1}^{\infty} \mathrm{Ca}^m h_m(z). \quad (5e)$$

In order to find the leading order approximation to the flow field and surface deformation, the additional simplifications of considering only the asymptotic limits of $\mathrm{Re} \to 0$ and $\mathrm{Pr} \to 0$, which correspond to the Stokes flow and conduction heat transport, respectively, are introduced. The latter situation arises, for example, in molten silicon ($\mathrm{Pr} = 0.023$). Both limits correspond to $\mathrm{Ma} \to 0$. With these assumptions the shape of the interface decouples from the flow field and is determined by the conditions of static equilibrium of an isothermal floating zone. Then, the temperature and flow fields can be determined separately by solving the governing equations with known location of the interface. Finally, the interface deformation is re-evaluated as a higher-order correction to the static shape.

Substituting these expansions into equations (3b, c), normal-stress condition (4c), volume constraint (4g) and contact line condition (4h), one obtains the problem of order Ca^{-1}, corresponding to a static meniscus problem [denoted by the subscript s in (5) and (6)]

$$\frac{\partial p_s}{\partial r} = 0, \quad (6a)$$

$$\frac{\partial p_s}{\partial z} = 0, \quad (6b)$$

with boundary conditions

$$-p_s = N_s^{-1}\left(N_s^{-2}\frac{\mathrm{d}^2 h_s}{\mathrm{d}z^2} - h_s^{-1}\right), \quad (6c)$$

$$\int_{-1}^{1} h_s^2 \mathrm{d}z = 2/A, \quad (6d)$$

$$h_s(-1) = h_s(1) = 1/A. \quad (6e)$$

In the case considered (i.e. zero gravity force), surface deformations cannot occur, the static shape is cylindrical with $h_s(z) = 1/A$, and the pressure jump $p_s = A$ is a constant. Note that the maximum length of a statically stable liquid zone is determined by the Rayleigh limit $A = \pi$ [17].

Inserting the expansion (5) into equations (3) and boundary conditions (4), and considering asymptotic limits of $\mathrm{Re} \to 0$ and $\mathrm{Pr} \to 0$, one obtains the problem of order of Ca^0, which corresponds to the following Stokes-type problem

$$u_{0r} + r^{-1}u_0 + w_{0z} = 0, \quad (7a)$$

$$-p_{0r} + \nabla^2 u_0 - r^{-2}u_0 = 0, \quad (7b)$$

$$-p_{0z} + \nabla^2 w_0 = 0, \quad (7c)$$

$$\nabla^2 T_0 = 0, \quad (7d)$$

with boundary conditions

$$z = \pm 1, \quad u_0 = w_0 = T_0 = 0, \quad (7e)$$

$$r = 0, \quad u_0 = w_{0r} = T_{0r} = 0, \quad (7f)$$

$$r = 1/A, \quad u_0 = 0, \quad (7g)$$

$$w_{0r} = -T_{0z}, \quad (7h)$$

$$T_{0r} = -4\mathrm{Bi}(T_0 - T_a). \quad (7i)$$

We note that determination of the temperature field is independent of the flow field, while the flow field is coupled to the temperature field through the tangential stress boundary condition (7h).

The temperature field (zero order)

The resulting problem is linear. The temperature field reduces to the solution of the axisymmetric conduction problem with boundary conditions (7e) and (7i). The solution is straightforward and is

$$T_0(r,z) = \sum_{k=0}^{+\infty} a_k I_0\left(\frac{2k+1}{2}\pi r\right)\cos\left(\frac{2k+1}{2}\pi z\right) \quad (8a)$$

where I_0 is the modified Bessel function of zero order, and the coefficients a_k are given by

$$a_k = \frac{4\mathrm{Bi}\int_{-1}^{1}\exp(-z^2/d^2)\cos\left(\frac{2k+1}{2}\pi z\right)\mathrm{d}z}{\frac{2k+1}{2}\pi I_1\left(\frac{2k+1}{2A}\pi\right) + 4\mathrm{Bi}I_0\left(\frac{2k+1}{2A}\pi\right)}. \quad (8b)$$

The convergence of this expression is extremely fast and two terms are sufficient to obtain an accurate result.

The velocity field (zero order)

Introduce an axisymmetric streamfunction Ψ, such that

$$u_0 = \Psi_z, \quad \text{and} \quad w_0 = -\Psi_r - r^{-1}\Psi. \quad (9a)$$

The velocity field at order Ca^0 reduces to the biharmonic differential equation for Ψ

$$(\nabla^2 - r^{-2})^2\Psi = 0, \quad (9b)$$

with the following boundary conditions

$$z = \pm 1, \quad \Psi = \Psi_z = 0, \quad (9c)$$

$$r = 1/A, \quad \Psi_z = (\nabla^2 - r^{-2})\Psi - T_{0z} = 0. \quad (9d)$$

Since the imposed temperature field in our case is even in z, $u_0 = \Psi_z$ must be even, so Ψ is odd. The solution of (9b) can be expressed in terms of the product function $I_1(rS_n)\phi_1^n(z)$ which is biharmonic and satisfies the boundary condition (9c). (For details, see Joseph *et al.* [9].) It is

$$\Psi(r,z) = \sum_{n=-\infty}^{+\infty} \frac{C_n}{S_n^2} I_1(rS_n)\phi_1^n(z) \quad (9e)$$

where I_1 is the modified Bessel function of first order and $\phi_1^n(z)$ is the odd Papkovich–Fadle functions associated with the eigenvalues S_n which are the non-zero roots of $\sin(2S_n) - 2S_n = 0$. (Note that all of the non-zero roots S_n are complex; these roots are ordered according to their increasing real parts.) The

odd functions $\phi^n = [\phi_1^n(z), \phi_2^n(z)]$ and $\Psi^n = [\Psi_1^n(z), \Psi_2^n(z)]$ are defined as

$$\phi_1^n(z) = S_n \cos(S_n)\sin(zS_n) - zS_n \sin(S_n)\cos(zS_n), \quad (10a)$$

$$\phi_2^n(z) = -\phi_1^n(z) + 2\sin(S_n)\sin(zS_n), \quad (10b)$$

$$\Psi_1^n(z) = \phi_1^n(z) + 2\sin(S_n)\sin(zS_n), \quad (10c)$$

$$\Psi_2^n(z) = \phi_1^n(z). \quad (10d)$$

The expansion coefficients C_n are found by projecting the boundary condition (9d)

$$\begin{bmatrix} \nabla^2 - r^{-2} \\ \partial_z^2 \end{bmatrix} \Psi(1/A, z) = \sum_{n=-\infty}^{+\infty} C_n I_1(S_n/A)\phi^n = \begin{bmatrix} T_{oz}(1/A, z) \\ 0 \end{bmatrix} \quad (11a)$$

onto the orthogonal vector functions Ψ^n using the bi-orthogonality condition

$$\int_{-1}^{1} \Psi^m \cdot \begin{bmatrix} 0 & -1 \\ 1 & 2 \end{bmatrix} \cdot \phi^n \, dz = -4\sin^4(S_n)\delta_{mn} \quad (11b)$$

where $\delta_{mn} = 0$ if $m \neq n$, and $\delta_{mn} = 1$ if $n = m$.

$$C_n = \frac{S_n^4 \sin^{-4}(S_n)}{I_1(S_n/A)} \sum_{k=0}^{\infty} (-1)^{k+1} a_k \frac{2k+1}{2}\pi I_0 \times \left(\frac{2k+1}{2}\pi\right)\left[\left(\frac{2k+1}{2}\pi\right)^2 - S_n^2\right]^{-2}. \quad (11c)$$

The expressions for the velocity components u_0, w_0, as deduced from (9a), are

$$u_0(r, z) = \sum_{n=-\infty}^{+\infty} \frac{C_n}{S_n} I_1(rS_n)[S_n \cos(S_n)\cos(zS_n) - \sin(S_n)\cos(zS_n) + zS_n \sin(S_n)\sin(zS_n)], \quad (12a)$$

$$w_0(r, z) = \sum_{n=-\infty}^{+\infty} \frac{C_n}{S_n} I_0(rS_n)\phi_1^n(z). \quad (12b)$$

The pressure field (zero order)

The pressure is a single valued function. According to Stokes' theorem,

$$p(b) - p(a) = \int_a^b p_r \, dr + p_z \, dz,$$

is independent of the path joining a to b, which allows us to write

$$p_0(r, z) = p_0(0, 0) + \int_0^r p_{0r}(r, 0)\, dr + \int_0^z p_{0z}(r, z)\, dz. \quad (13a)$$

Calculating p_{0r} and p_{0z} from equations (7b) and (7c), respectively, one obtains

$$p_0(r, z) = 2 \sum_{n=-\infty}^{+\infty} C_n \sin(S_n) \times [I_0(rS_n)\cos(zS_n) - 1]. \quad (13b)$$

Note that the pressure is normalized in such a way that $p_0(0, 0) = 0$.

Higher order solution

For $\mathrm{Re} \neq 0$ and $\mathrm{Pr} \neq 0$, the solution for the flow field has the form:

$$u(r, z) = u_0(r, z) + \mathrm{O(Ca, Re, Pr)}, \quad (14a)$$

$$w(r, z) = w_0(r, z) + \mathrm{O(Ca, Re, Pr)}, \quad (14b)$$

$$T(r, z) = T_0(r, z) + \mathrm{O(Ca, Re, Pr)}, \quad (14c)$$

$$p(r, z) = Ca^{-1}A + p_0(r, z) + \mathrm{O(Ca, Re, Pr)}. \quad (14d)$$

Small surface deformations (first order)

The first order surface deformation of the liquid zone is calculated by considering equations (4c), (4g) and (4h) at $\mathrm{O(Ca^1, Re^0, Pr^0)}$

$$h_{1zz} + A^2 h_1 = (2u_{0r} - p_0 + AT_0)r = 1/\mathrm{A}, \quad (15a)$$

$$\int_{-1}^{1} h_1 \, dz = 0, \quad (15b)$$

$$h_1(-1) = h_1(1) = 0. \quad (15c)$$

The pressure p_0 in equation (15a) consists of two components, $p_0 = \tilde{p} + \tilde{C}$, in which $\tilde{p}$ is the pressure determined by equation (13b), and $\tilde{C}$ is an arbitrary additive constant to be determined from the volume constraint (4g).

Substituting u_0, p_0 and T_0 from equations (12a), (13b) and (8a), respectively, into equation (15a), one obtains

$$h_1(z) = \sum_{n=-\infty}^{\infty} [B_{1n} z \sin(zS_n) + B_{2n}\cos(zS_n)] + \sum_{k=0}^{\infty} B_{3k}\cos\left(\frac{2k+1}{2}\pi z\right) + \frac{B_4}{\sin(A) - A\cos(A)} A\cos(Az) - \tilde{C}, \; A \neq \tan(A), \quad (16)$$

with

$$B_{1n} = \frac{2C_n S_n \sin(S_n)\left[I_0(S_n/A) - \frac{A}{S_n} I_1(S_n/A)\right]}{A^2 - S_n^2},$$

$$B_{2n} = \frac{2C_n \left\{\left[I_0(S_n/A) - \frac{A}{S_n} I_1(S_n/A)\right][S_n \cos(S_n) - \sin(S_n)] - I_0(S_n/A)\sin(S_n)\right\} - 2B_{1n}S_n}{A^2 - S_n^2},$$

$$B_{3k} = \frac{a_k I_0\left(\frac{2k+1}{2}\pi\right)}{A^2 - \left(\frac{2k+1}{2}\pi\right)^2},$$

$$B_4 = \sum_{n=-\infty}^{\infty}\left[\left(B_{1n} - \frac{B_{1n}}{S_n^2} - \frac{B_{2n}}{S_n}\right)\sin(S_n) + \left(B_{2n} + \frac{B_{1n}}{S_n}\right)\cos(S_n)\right] - \sum_{k=0}^{\infty}(-1)^k B_{3k}\left(\frac{2k+1}{2}\pi\right)^{-1},$$

$$\tilde{C} = \frac{B_4}{\sin(A) - A\cos(A)} A\cos(A) + \sum_{n=-\infty}^{\infty}[B_{1n}\sin(S_n) + B_{2n}\cos(S_n)].$$

RESULTS OF CALCULATIONS

In this section we present the calculated results of flow field and surface deformations described by the above analytical expressions. For a practical evaluation of Ψ, u_0, w_0, p_0, T_0 and h_1 the sums over n and k have to be truncated at order N and K, respectively. Here N was chosen in such a way that the results for order $N+1$ did not deviate from those at order N by more than about 1% of the maximum absolute value of w_0. Taking $K = 1$, i.e. two terms for the calculation of sums over k, gives sufficiently accurate results.

The flow pattern and temperature field, for aspect ratio $A = 1$ and Biot number $\mathrm{Bi} = 0.5$, are shown in Fig. 2. (The streamlines represent lines of $r\Psi =$ const.) The highest temperature occurs at midsection of the zone, and the lowest at both endwalls with $T_0 = 0$. Thus, the maximum of surface tension appears at the endwalls and the minimum at the free surface center. The liquid is therefore driven along the surface from center to side wall and returns along the axis, forming two counter-rotating toroidal vortices. The flow cells are symmetric about the midsection with each cell center near the free surface; this is due to the symmetry of thermal boundary condition. This typical flow configuration is well known from experimental work and numerical simulations [16].

The surface deformation h_1, defined by equation (16) for a floating zone of aspect ratio $A = 1$, and Biot number $\mathrm{Bi} = 0.5$, is illustrated in Fig. 3. The deformation is symmetric about the midsection with the surface bulging at the endwalls [$h_{1\max}(z) = 0.49 \times 10^{-2}$] and constricting at the center [$h_{1\min}(z) = -0.39 \times 10^{-2}$]. Such a deformation is a result of two competing effects. The first is a dynamic effect

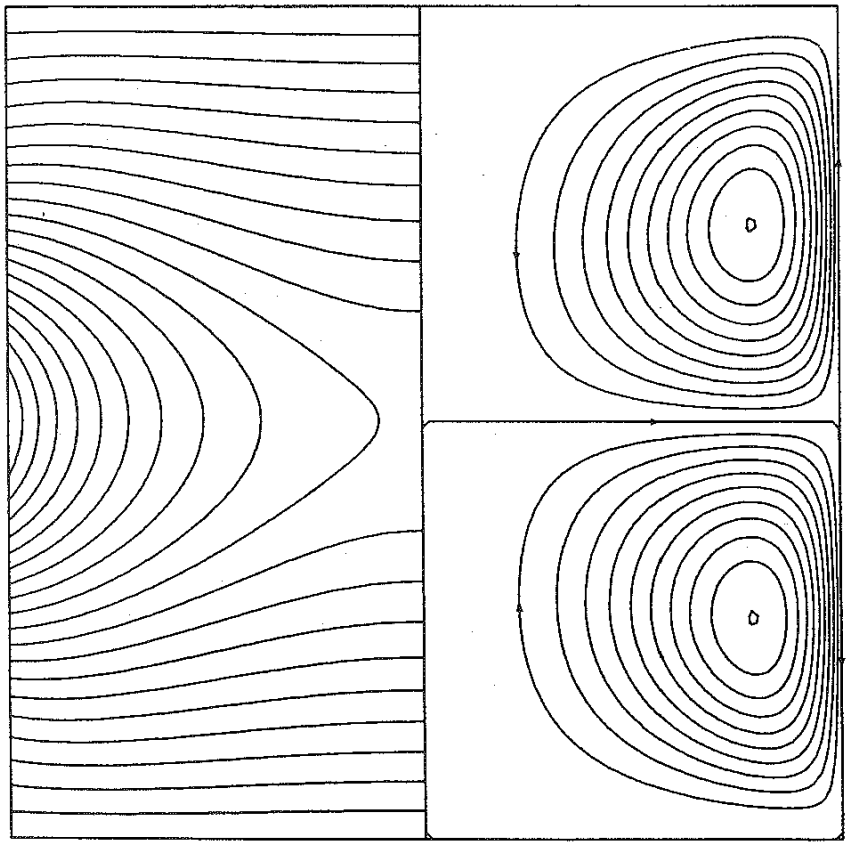

Fig. 2. Stream function (right half) and temperature contours (left half) in a floating zone for $A = 1$ and $\mathrm{Bi} = 0.5$. The contours are equally spaced between the maximum and the minimum values of the variable concerned: $\Psi_{\max} = 8.89 \times 10^{-3}$ and $\Psi_{\min} = -8.89 \times 10^{-3}$, and $T_{0\max} = 0.575$ and $T_{0\min} = 0$, respectively.

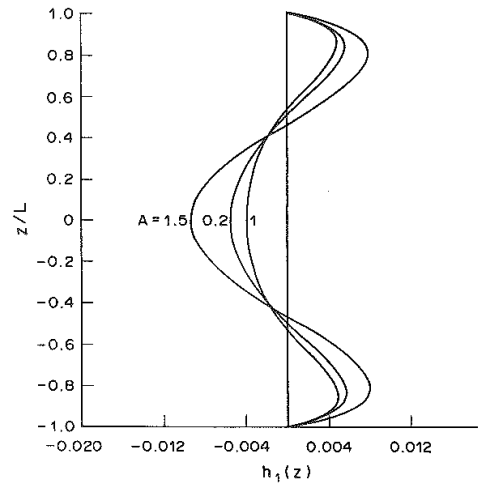

Fig. 3. Surface deformation $h_1(z)$ for various aspect ratios.

associated with the motion of the liquid which is generated by thermocapillarity (condition 4d); the induced pressure gradient gives rise to a higher pressure at the endwalls that causes the fluid to return. The second effect is due to a capillary pressure that results from the variation in surface tension (condition 4c). The former effect is stronger in the present case and leads to the above deformation. When the aspect ratio A is varied, the qualitative form of the deformation remains the same, as in the case of $A = 1$, while its amplitude increases. The form and dependence on A of the deformation h_1 well consist with the numerical results given by Rybicki and Floryan [17]. (The variation of surface deformations with aspect ratio is discussed subsequently.) In the following section the influence of Biot number and aspect ratio on the flow field is analyzed.

Influence of Biot number (in the limit case $Ma \to 0$)

Since the zone is subjected to the heat flux condition and the liquid gains energy from the heater by radiation, the influence of the Biot number, which measures the heat transfer between the liquid and ambient gas, on the temperature field is obviously strong. Its influence on the velocity field is also expected to be strong because thermocapillary forces are directly connected to the surface temperature distribution. Figure 4 displays the variations of the maximum dimensionless surface temperature and surface velocity, as a function of Biot number for various aspect ratios. For $\mathrm{Bi} < 0.1$, the maximum surface temperature and maximum surface velocity increase linearly with increasing Biot number. The asymptotic values would be obtained when Biot number is larger than 10 with maximum surface temperature $T_{0\max} \approx 1$ and maximum surface velocity $w_{0\max} \approx 0.2$. Indeed, from equations (8a) and (8b) one can obtain following approximations for surface temperature and surface velocity

$$T_0(1/A, z) \approx \mathrm{Bi}\left[\frac{3\cos(\pi/2z)}{0.96\,A^{-1/3} + 4\mathrm{Bi}} + \frac{\cos(3\pi/2z)}{4.2\,A^{-1/3} + 4\mathrm{Bi}}\right], \tag{17a}$$

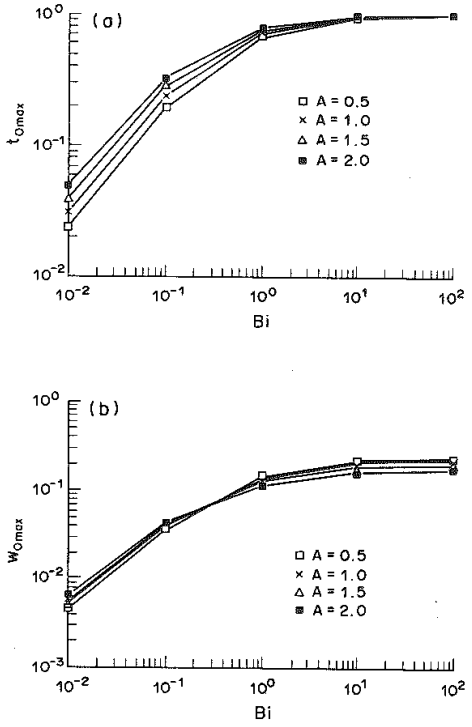

Fig. 4. Biot number dependence of (a) maximum temperature $T_{0\max}$ and (b) maximum axial velocity $w_{0\max}$ at the free surface ($r = 1/A$) for various aspect ratios.

$$w_0(1/A, z) \approx -f(A)T_{0z}(1/A, z) \approx f(A)\frac{3\pi}{2} \times \mathrm{Bi}\left[\frac{\sin(\pi/2z)}{0.96A^{-1/3} + 4\mathrm{Bi}} + \frac{\sin(3\pi/2z)}{4.2\,A^{-1/3} + 4\mathrm{Bi}}\right], \tag{17b}$$

In relation (17b), $f(A)$ is a function which can be expressed analytically in terms of the aspect ratio A. It was found that for moderate aspect ratios, say $0.2 < A < 3$, expressions (17a) and (17b) accurately described the surface temperature and surface velocity. Furthermore, setting $z = 0$ in equation (17a) and $z = 0.5$ in equation (17b) yields the maximum surface temperature and maximum surface velocity, respectively.

Influence of aspect ratio (in the limit case $Ma \to 0$)

Here, the influence of aspect ratio on velocity field and surface deformation is discussed. The dimensionless axial velocity w_0 described by equation (12b) decreases with increasing aspect ratio. Expanding w_0 of equation (12b) for small $1/A$ ($A \to \infty$) yields

$$w_0(r, A) = -\text{const}\; T_{0z}(r, A)\frac{A}{2}\left(r^2 - \frac{1}{2A^2}\right). \tag{18}$$

This result is identical to the Hagen–Poiseuille profile given by Xu and Davis [15] if $T_{0z} = -1$.

Variation of the maximum $h_{1\max}$ of the surface deformation with the decrease of the aspect ratio A, for Biot number $\mathrm{Bi} = 0.5$, is displayed in Fig. 5. The

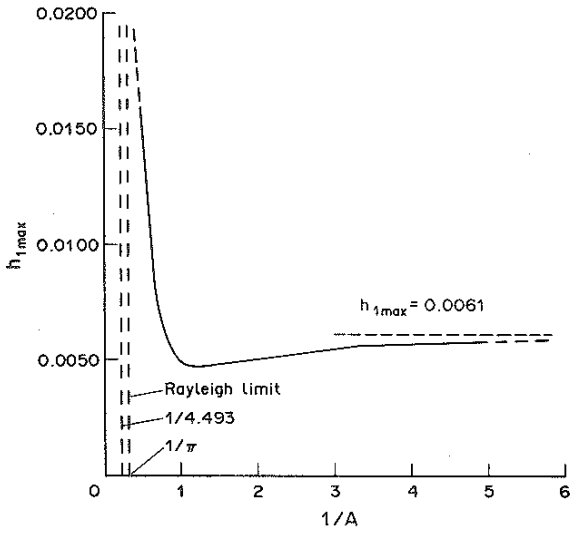

Fig. 5. Variation of the maximum surface deformation $h_{1\max}$ with decrease of aspect ratio A for Bi = 0.5.

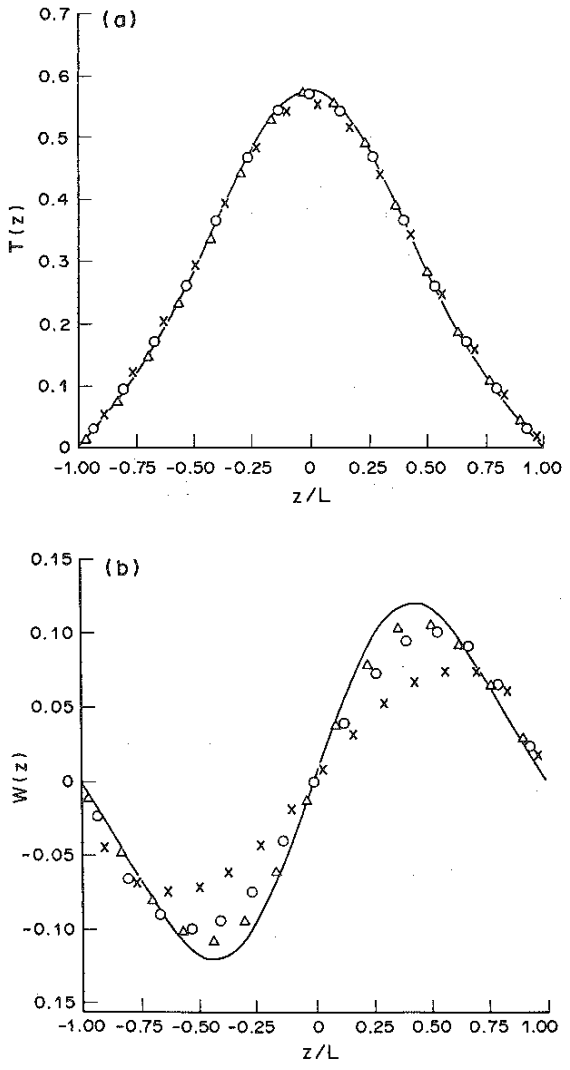

Fig. 6. Axial dependence of (a) temperature and (b) axial velocity at the free surface for $A = 1$, Bi = 0.5, Pr = 0.023 and Ca = 10^{-3}. Full lines are the analytical results $T_0(z)$ and $w_0(z)$. Symbols represent the numerical results for Ma = 2 (symbol = Δ), Ma = 10 (symbol = ○) and Ma = 50 (symbol = ×), respectively.

amplitude of the deformation $h_{1\max}$ at first decreases and then increases towards an asymptotic state with $h_{1\max} = 0.0061$ as $1/A \to \infty$. Minimum of $h_{1\max}$ corresponds to the aspect ratio $A = 1$. When $A \to 4.4934$ [largest root of $A = \tan(A)$ in equation (16)], the amplitude of the deformation increases without limit, and small deformation assumption obviously is no longer valid. However, at $A = \pi$ capillary instability sets in and it should lead to a breakup of the floating zone.

COMPARISON WITH NONLINEAR NUMERICAL CALCULATIONS

In this section the present analytical solution is compared with recent non-linear numerical solutions in which the surface deformations are taken into account [15]. Surface temperatures and surface axial velocities are shown in Fig. 6(a) and (b), for $A = 1$, Bi = 0.5, Pr = 0.023 and three different Marangoni numbers, Ma = 2, 10, 50. The numerical results tend to the analytical ones, asymptotically in the limit Ma → 0. The temperature field is nearly identical to the numerical one for Marangoni number as large as 300 (Pr = 0.023), but the velocity field approximation looses its validity for Marangoni numbers larger than 10, as indicated by numerical result shown in Fig. 6(b). The Prandtl number dependence of the surface temperature is shown in Fig. 7, for Re = 500, $A = 1$, Bi = 0.5 and three different Prandtl numbers, Pr = 0.01, 0.1, 1. One sees that for Prandtl numbers less than 0.1 the temperature field is dominated by conduction and for larger Pr, the coupling between the temperature field and velocity field becomes significant.

A comparison for the surface deformation is shown in Fig. 8, for $A = 1$, Bi = 0.5, Pr = 0.1, Ca = 10^{-3}. For small Marangoni numbers, say Ma ⩽ 2, the results from the analytical solution and numerical calculation are nearly identical. However, for larger Marangoni number the numerical results differ significantly as indicated in Fig. 8. The tendency of the

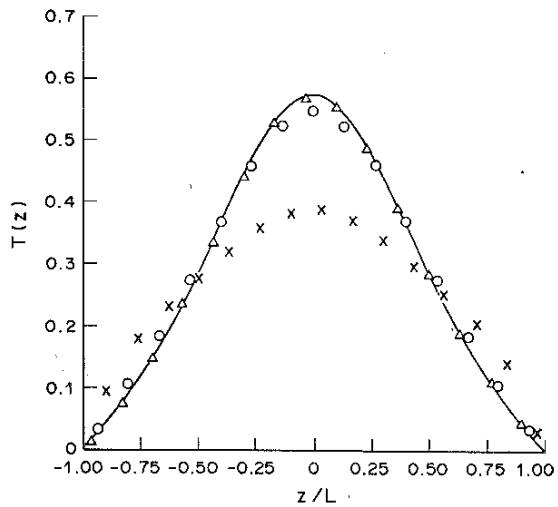

Fig. 7. Prandtl number dependence of temperature at the free surface for Re = 500, $A = 1$, Bi = 0.5 and Ca = 10^{-3}. Full lines are the analytical results $T_0(z)$. Symbols represent the numerical results for Pr = 0.01 (symbol = Δ), Pr = 0.1 (symbol = ○) and Pr = 1 (symbol = ×), respectively.

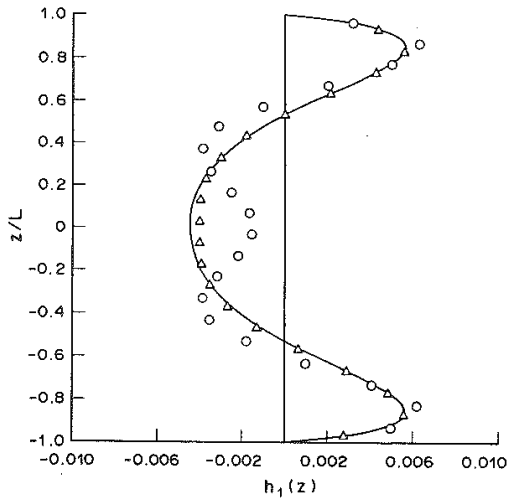

Fig. 8. Surface deviation from its original cylindrical shape, for $A = 1$, Bi = 0.5. Full line is the analytical result $h_1(z)$. Symbols represent the numerical results of $[h(z) - 1/A]/\mathrm{Ca}$ for Pr = 0.1, Ca = 10^{-3}, Ma = 2 (symbol = Δ) and Ma = 10 (symbol = ○), respectively.

surface in the center of the zone is to curve outward as the Marangoni number is increased.

FINAL REMARKS

The importance of the oscillatory thermocapillary convection for crystal growth from the melt in floating zones has been known for a long time. However, the critical issues, such as the Marangoni number for a given aspect ratio at which the steady axisymmetric thermocapillary flow becomes time-dependent has not yet been accurately determined by numerical studies. Experimental studies of low Prandtl number melts are now lacking and more activity in this area is essential. A detailed study locating the critical values for the onset of oscillatory thermocapillary convection in floating zones is in progress using the present analytical solution as the basic steady solution in a bifurcation analysis [19].

Acknowledgements—We are grateful for comments from Professor Robert Sani (University of Colorado-Boulder, U.S.A.). This work is being supported by the Centre National d'Etudes Spatiales (Division Matériaux et Microgravité). The computations were carried out on IBM 3090-VF of CNUSC.

REFERENCES

1. J. L. Duranceau and R. A. Brown, *J. Crystal. Growth* **75**, 367 (1986).
2. A. Eyer, H. Leiste and R. Nitsche, *J. Crystal Growth* **71**, 173 (1985).
3. D. Schwabe, *PhysicoChem. Hydrody.* **2**, 263 (1981).
4. S. H. Davis, *Ann. Rev. Fluid Mech.* **19**, 403 (1987).
5. D. Schwabe, in *CRYSTALS 11* (Edited by H. C. Freyhardt), p. 76. Springer, Berlin (1988).
6. I. Da-Riva and E. A. Pereira, *Acta Astronautica* **9**, 217 (1982).
7. R. C. T. Smith, *Aust. J. Sci. Res.* **5**, 227 (1952).
8. D. D. Joseph and L. D. Sturges, *SIAM J. Appl. Math.* **34**, 7 (1978).
9. D. D. Joseph, L. D. Sturges and W. H. Warner, *Arch. Rational Mech. Anal.* **78**, 223 (1982).
10. L. G. Napolitano and C. Golia, Effects of gravity levels on Marangoni Stokes flows in Plateau configurations, *Acta Astronautica* **11**, 213 (1984).
11. L. G. Napolitano, C. Golia and A. Viviani, Effects of non-linear tension on combined free-convection in cavities, *L'Aerotecnica Missili Spazio* **63**, 29 (1984).
12. A. M. J. Davis, Thermocapillary convection in liquid bridges: solution structure and eddy motions, *Phys. Fluids* **A1**, 475 (1989).
13. H. Kuhlmann, *Phys. Fluids A* **1**, 672 (1989).
14. S. C. Hardy, *J. Crystal Growth* **69**, 456 (1984).
15. G. Chen and B. Roux, *Adv. Res. Space*. To be published.
16. A. Rybicki and J. M. Floryan, *Phys. Fluids* **30**, 1956 (1987).
17. A. Rybicki and J. M. Floryan, *Phys. Fluids* **30**, 1973 (1987).
18. J. J. Xu and S. H. Davis, *Phys. Fluids* **26**, 2880 (1983).
19. B. Roux, G. de Vahl Davis, M. Deville, R. L. Sani and K. H. Winters, in *Notes on Numerical Fluids Mechanics* (Edited by Vieweg), Vol. 27, p. 285 (1990).

APPENDIX

Nomenclature

A = aspect ratio, L/R
Bi = Biot-like number, $\epsilon\sigma^*(T_m)^3L/\kappa$
Ca = capillary number, $\gamma\Delta T/\sigma_0$
$h(z)$ = dimensionless melt–gas interface shape
L = half floating zone height
Ma = Marangoni number, RePr
$p(r, z)$ = dimensionless pressure field
Pr = Prandtl number, ν/α
R = crystal (and rod) radius
Re = Reynolds number, $\gamma\Delta T/\mu\nu$
r, z = dimensionless radial and axial coordinates
$T(r, z)$ = dimensionless temperature field
$T_a(z)$ = ambient temperature
T_m = melting temperature
$u(r, z)$ = dimensionless radial velocity component
$w(r, z)$ = dimensionless axial velocity component

Greek symbols

α = thermal diffusivity
γ = surface tension derivative, $-\partial\sigma/\partial T$
ϵ = emissivity
κ = thermal conductivity
ΔT = maximum temperature difference
μ = viscosity
ν = kinematic viscosity
ρ = density
σ = surface tension
σ^* = Stefan–Boltzmann constant
Ψ = dimensionless streamfunction

Subscripts

r, z = partial derivatives
s = static values